Noise-induced leakage and counting errors in the electron pump

R. L. Kautz, Mark W. Keller, and John M. Martinis
National Institute of Standards and Technology, 325 Broadway, Boulder, Colorado 80305
(Received 15 June 2000)

Computer simulations reveal that the lowest rates of leakage and counting errors observed in the electron pump can be explained by photon-assisted tunneling driven by $1/f$ noise. The noise power at microwave frequencies required to account for the observed errors is consistent with extrapolation of the low-frequency noise spectrum commonly recorded in single-electron transistors. Pump simulations, based on the ground-capacitance model, include cotunneling as well as single-junction photon-assisted tunneling. Quantitative agreement between theory and experiment is obtained for leakage and counting errors in pumps with four, five, six, and seven junctions in the limit of low temperatures and low counting rates. The effect of self-heating is explored.

I. INTRODUCTION

The electron pump, a circuit first demonstrated by Pothier *et al.* in 1991,[1] uses the Coulomb blockade in nanoscale tunnel junctions to control the transfer of electrons one-by-one between input and output electrodes. Provided errors are infrequent, the electron pump has potential applications in metrology as a standard of either current[1] or capacitance.[2] In 1996, measurements[3] of a well-characterized seven-junction pump demonstrated a leakage rate in the hold mode of 3×10^{-4} electrons per second (e/s) and a relative counting error of 1.5×10^{-8}, permitting the recent demonstration of a capacitance standard with metrological accuracy.[4] Although small, the experimental leakage and counting errors of the seven-junction pump exceed predictions of the orthodox theory of single-electron tunneling by 17 and 12 orders of magnitude, respectively.[5,6] These discrepancies could be explained if the temperature of the pump were significantly higher than that of the substrate, but in the case of leakage this possibility was ruled out by a direct measurement of the electron temperature in the hold mode.[5] Thus, leakage in the seven-junction pump is due to a mechanism not contained in the orthodox theory, including cotunneling.

Photon-assisted tunneling, associated either with environmental noise[7] or the cyclic bias,[8] has been suggested as a possible source of errors in electron pumps. While experimental tests have ruled out room-temperature noise introduced through the bias leads as a problem in well-shielded pump experiments,[5] numerous measurements of single-electron transistors (SET's) have established the existence of $1/f$ noise, intrinsic to the devices, associated with charge motion in the dielectric material.[9–21] Can dielectric charge motion produce sufficient noise to explain the errors observed in the pump? Recent calculations reveal that the level of noise at microwave frequencies required to explain the measured leakage in four- and six-junction pumps is consistent with an extrapolation of the $1/f$ noise measured at audio frequencies in SET's.[22] This observation suggests that charge noise in the dielectric may be the primary cause of errors in the pump, although it falls far short of proving the case. Here, we present additional evidence based on a comparison of calculated noise-induced leakage and counting errors with previous measurements[3,6,23] in five- and seven-junction pumps. Over the measured ranges of temperature and pumping speed, we generally obtain good agreement between theory and experiment, assuming $1/f$-noise levels typical of those in SET's.

To date, the observation of $1/f$ noise in SET's has been restricted to frequencies less than about 1 kHz. Does $1/f$ noise persist at frequencies up to roughly 30 GHz, as required to explain pump errors by photon-induced tunneling? Although no definitive answer is given, in Sec. II we describe a scenario that makes plausible the existence of charge noise at microwave frequencies. Assuming such $1/f$ noise, we proceed in Sec. III to calculate the leakage rate of a pump in the hold mode, using the ground-capacitance model, and compare with experiment. In Sec. IV, we present similar results for noise-induced counting errors as a function of both temperature and pumping speed and identify the dominant error mechanisms in the five- and seven-junction pumps. In Sec. V, we consider the possibility that elevated temperatures due to self heating also contribute to counting errors.

II. CHARGE NOISE

In the limit of weak noise, Martinis and Nahum derived an expression for the photon-assisted tunneling rate Γ_N due to single-photon noise processes[7]

$$\Gamma_N(\Delta E)=\frac{\pi}{R_K}\int_{-\infty}^{\infty}\frac{S_V(|\varepsilon|/\hbar)\Gamma_0(\Delta E-\varepsilon)}{\varepsilon^2}d\varepsilon, \qquad (1)$$

where ΔE is the change in electrostatic energy associated with tunneling, $S_V(\omega)$ is the power spectral density of the noise voltage V appearing across the junction, and Γ_0 is the tunneling rate in the absence of noise,

$$\Gamma_0(\Delta E)=\frac{-\Delta E/e^2R_J}{1-\exp(\Delta E/k_BT)}. \qquad (2)$$

Here, e is the elementary charge, $h=2\pi\hbar$ is the Planck constant, k_B is the Boltzmann constant, T is the temperature, $R_K=h/e^2$ is the resistance quantum, and R_J is the tunneling resistance. Equation (1) is valid provided $\Delta E>k_BT$ and the

embedding impedance of the junction is much less than the resistance quantum. If we further assume that the noise follows a $1/f$ spectrum, $S_V = 2\pi\alpha/\omega = \alpha/f$, and that Γ_0 can be replaced by its zero-temperature limit

$$\Gamma_0(\Delta E) = \begin{cases} \dfrac{|\Delta E|}{e^2 R_J} & (\Delta E < 0), \\ 0 & (\Delta E > 0) \end{cases} \tag{3}$$

then we obtain for the noise-induced tunneling rate[22]

$$\Gamma_N(\Delta E) = \frac{\pi\alpha}{R_J}\int_{\Delta E}^{\infty} \frac{\varepsilon - \Delta E}{\varepsilon^3} d\varepsilon$$

$$= \frac{\pi\alpha}{2R_J \Delta E} \quad (\Delta E > k_B T). \tag{4}$$

This simple formula underlies all of the noise-induced tunneling effects to be considered in this paper. Note that the only portion of the noise spectrum contributing to Γ_N is that for which $\varepsilon = \hbar\omega > \Delta E$. Since typical Coulomb barriers in the pump are of order $\Delta E = 0.1$ meV, the relevant noise frequencies are of order 25 GHz.

The noise spectrum $S_V = \alpha/f$, used to derive Eq. (4), is completely characterized by the constant α. To evaluate α, we turn to experimental measurements of SET noise, in which the $1/f$ component is typically evaluated around 10 Hz. When the charge noise at the input is translated into voltage noise across the junctions, a variety of SET experiments yield values for $\sqrt{\alpha}$ ranging from 30 nV to 3 μV.[9–21] This ballpark range for α provides a standard against which we will compare the noise required to explain errors in the electron pump.

The question that remains to be considered is whether the $1/f$ noise observed at audio frequencies in the SET actually extends to the microwave region. First we note that, while SET noise is expected to be dominated by shot noise at high frequencies, this source of noise is not relevant to the pump. Shot noise is due to the discrete charges that make up the tunnel current and is proportional to this current. Because the pump operates at zero current, except for the distinct tunneling events accounted for in the theory of its operation, shot noise does not contribute to photon-induced tunneling in the pump. The real question is whether the charge motion that gives rise to low-frequency $1/f$ noise in the SET includes components at microwave frequencies.

The origin of $1/f$ noise in the SET is often attributed to the presence of thermally activated two-level fluctuators (TLF's): charges moving back and forth between trap sites in response to thermal noise. The dynamics of a single TLF is modeled by the motion of a particle in a potential with two minima, as shown in Fig. 1. The mean time t_e for thermally induced escape from the left-hand well is

$$t_e = \frac{2\pi}{\omega_0}\exp(\Delta U/k_B T), \tag{5}$$

where ω_0 is the angular attempt frequency and ΔU is the depth of the well. In the case of a symmetric potential with $\omega_0' = \omega_0$ and $\Delta U' = \Delta U$, thermally induced motion between the two wells yields a random telegraph signal with a Lorentzian power spectrum of the form

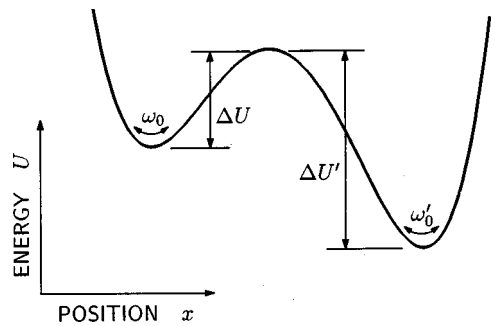

FIG. 1. Model potential for a two-level fluctuator.

$$S(\omega) = \frac{S(0)}{1 + (\omega t_e/2)^2}. \tag{6}$$

As described by Dutta and Horn,[24] an ensemble of such TLF's with a uniform distribution of activation energies ΔU gives rise to a $1/f$ spectrum. Thus, $1/f$ noise in the SET might result from thermally activated TLF's, corresponding to motion of charges between trap sites in the dielectric, and several authors have directly observed the expected random telegraph signals.[9,10,12,13,16,17,25]

However, other experimental evidence suggests that an ensemble of thermally activated TLF's is not the primary cause of $1/f$ noise in the SET. This possibility is important here because TLF's cannot generate photons at frequencies above roughly $f = k_B T/h$, or about 600 MHz at 30 mK. [A maximum frequency follows from Eq. (5), given that ΔU must be greater than $\hbar\omega_0/2$ to bind a charge in the potential well.] That is, the noise required to explain pump errors cannot derive from a source in thermal equilibrium at 30 mK. Perhaps not coincidentally, there is evidence that the $1/f$ noise in SET's is not of an equilibrium nature. Although the random telegraph noise observed at low frequencies in SET's is persistent and represents an equilibrium effect, it is usually associated with a distinct Lorentzian lying above the $1/f$ curve. The nonequilibrium nature of the $1/f$ noise is shown directly by the fact that the $1/f$ portion of the noise spectrum is observed to decay gradually in the days and weeks after the SET is cooled. For the case illustrated in Fig. 2, the charge noise at 10 Hz decays by more than a factor of 2 over a period of 12 days, and a similar decay is observed each time the device is cooled. These observations suggest that $1/f$ noise derives from the slow release of energy trapped in metastable charge states when the device is rapidly cooled from room temperature. In this scenario, $1/f$ noise is a by-product of a slow relaxation process that gradually brings charges to minimum-energy equilibrium positions.

In the case of thermally activated TLF's, $1/f$ noise can be generated by a small number of charge traps that might be located in the barriers of the tunnel junctions. In contrast, if the noise is due to a charge relaxation process, a large number of traps must be involved, since a given trap is unlikely to participate more than once. Thus, it is significant that recent observations of noise correlations between neighboring junctions indicate that the charge noise in SET's originates in the substrate rather than the junction barriers.[14,15] Since the

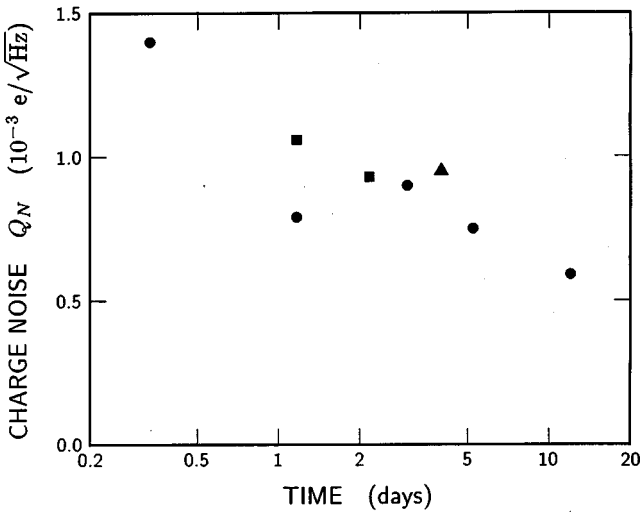

FIG. 2. Charge noise at 10 Hz for a SET as a function of the time after the device reached a temperature of 4 K. The SET used $Al/AlO_x/Al$ junctions fabricated on a fused-silica substrate, with junction resistances of 30 kΩ and capacitances of about 1 fF. The SET was operated in the normal state at about 40 mK, with a magnetic field applied to suppress superconductivity. Data for the same device are shown for three different cooling runs, indicated by circles, squares, and triangles.

volume of the substrate is orders of magnitude larger than that of the tunnel barriers, there is ample room for a large number of traps.

Additional evidence for nonequilibrium charge motion is provided by a study of the drift in the gate offset charge of a SET. In particular, Zimmerman and Huber have observed that fluctuations in the offset charge decay gradually over a period of days or weeks.[26] Assuming that $1/f$ noise is due to the motion of charges trapped in the substrate, fluctuations in the gate offset charge are probably a lower-frequency manifestation of the same charge motion that produces SET noise at 10 Hz. Thus, the decay of charge-offset fluctuations supports the nonequilibrium nature of $1/f$ noise. Finally, if $1/f$ noise is due to a slow relaxation of charge rather than thermally activated TLF's, then $1/f$ noise should not be a strong function of temperature as implied by Eq. (5) for a TLF. In fact, two studies find that the SET noise at 10 Hz is nearly independent of temperature below 100 or 200 mK.[12,15] Thus, as anticipated by Martinis *et al.*[23] and Zorin *et al.*,[14] the charge noise in single-electron circuits appears to be a nonequilibrium effect involving a large number of charges trapped in metastable states that move as they decay to lower energy states over a period of days or weeks.

If this charge-relaxation scenario is correct, then the $1/f$ noise spectrum could extend into the microwave region because the noise energy does not derive from a thermal source. In terms of the model potential shown in Fig. 1, we can imagine that ΔU is only marginally greater than k_BT so that escape from the left-hand well is likely to occur over a period of days, while $\Delta U'$ is much greater than k_BT, allowing production of microwave photons when escape occurs. Thus, provided charge traps exist with appropriate values of ΔU, we can obtain charge noise spanning a wide range of frequencies from the relaxation process. With regard to high frequencies, we note that attempt frequencies for dielectric

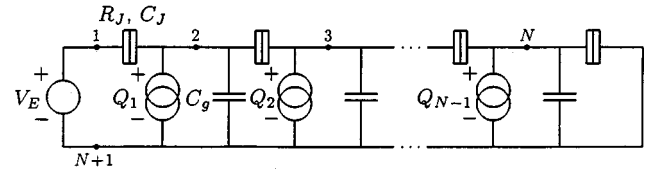

FIG. 3. Equivalent circuit for the electron pump within the ground-capacitance model. Nanoscale tunnel junctions are indicated by boxes.

charge traps are typically of order 10^{12} Hz,[27] while the observation of low-frequency TLF's at 30 mK assures the existence of traps with sufficiently low ΔU. Thus, a nonequilibrium process could easily give rise to noise extending well into the microwave region.

How might the charge-relaxation scenario lead to a $1/f$ noise spectrum? One possibility assumes that, due to electrostatic interactions, the motion of a charge at one site will modify the potential elsewhere in the dielectric and trigger the motion of charges at other sites. In this case, charge relaxation might occur through a series of avalanches of various sizes. As Bak *et al.* have shown,[28] the correlations generated by a distribution of avalanche sizes can lead to a characteristic $1/f$ spectrum. If this mechanism explains the $1/f$ noise observed near 10 Hz, then it might well extrapolate to the microwave region.

While the charge-relaxation scenario is speculative, it does provide a plausible explanation for the microwave noise required to explain errors in the electron pump. At the same time, most of the conclusions reached in the following sections are independent of the presumed source of noise.

III. LEAKAGE

When operated as a capacitance standard, the pump is used to transfer a given number of electrons to a capacitor, then biased in the hold mode while the capacitor's voltage is measured. Because the measurement is affected by any leakage that occurs while the pump is in the hold mode, leakage current is an important pump parameter. The absolute leakage current I_A is measured by connecting the pump to an external capacitor, setting the pump bias voltages to zero, and counting the total number of leakage charges, either positive or negative, to reach the external capacitor over a period of time. While values of I_A as small as $3\times10^{-4}e/s$ have been recorded for a seven-junction pump,[5] theoretical predictions based on the orthodox theory of single-electron tunneling, with cotunneling included, yield $I_A=2\times10^{-21}e/s$.[5,6] Here we explain this discrepancy in terms of photon-assisted tunneling driven by microwave noise.

The circuit model of the electron pump used in the present calculations is shown in Fig. 3. The circuit consists of N nanoscale tunnel junctions connected in series to create $N-1$ isolated islands, labeled as nodes 2 through N in the figure. The junction capacitances C_J and resistances R_J are assumed to be identical. Each island has a capacitance C_g to ground and is biased by an independent charge source Q_i. In this ''ground-capacitance'' model, the capacitors C_g include the capacitance of the gate electrodes used to bias the islands plus parasitic island capacitances. Because the external ca-

pacitor is much larger than C_J or C_g, it is approximated here by a voltage source V_E.

A. Orthodox theory

Several authors have previously calculated the leakage of a series array of tunnel junctions in the absence of noise, using the orthodox theory of single-electron tunneling,[29] with cotunneling included.[6,30–33] Orthodox theory formulates the dynamics of the pump in terms of the probabilities P_n that the pump occupies a charge state n and the rates $\Gamma_{n'n}$ of transition between states n and n'. The index n specifies the charge on each of the $N-1$ islands of the pump. The probabilities of various charge states evolve according to

$$\frac{dP_n}{dt}=\sum_{n'\neq n}(\Gamma_{nn'}P_{n'}-\Gamma_{n'n}P_n), \tag{7}$$

where the first term accounts for the increase in P_n due to transitions from n' to n and the second term accounts for the decrease due to transitions from n to n'. In this transition-state picture, the ensemble average of the current through junction J at any instant is

$$I_J=e\sum_{n,n'}P_n[\Gamma^+_{n'n}(J)-\Gamma^-_{n'n}(J)], \tag{8}$$

where the $\Gamma^+_{n'n}(J)$ are the rates of transitions in which a charge moves in the positive direction through junction J, and the $\Gamma^-_{n'n}(J)$ are the rates of transitions in which a charge moves in the negative direction through junction J.

Equations (7) and (8) allow us to solve for the probabilities and currents provided the rates $\Gamma_{n'n}$ can be calculated. In general, $\Gamma_{n'n}$ includes contributions from an infinite number of processes that take the system from charge state n to n'. All multijunction cotunneling processes can be broken into a sequence of single-junction tunneling events, and, following Jensen and Martinis,[31] we specify a process by a list of integers $(j_1,j_2,\ldots,j_m)$. Here, each j_i is a number in the range $\pm1,\pm2,\ldots,\pm N$ that specifies the junction and the direction of tunneling for each event in the sequence. The process $(j_1,j_2,\ldots,j_m)$ is said to be an mth-order process because m single-junction events are included. Schematically, a third-order process for a transition from charge state n to n' can be diagrammed as follows:

$$\begin{array}{lccccccc}
\text{event:} & & j_1 & & j_2 & & j_3 & \\
\text{state:} & n & \rightarrow & s_1 & \rightarrow & s_2 & \rightarrow & n', \\
 & & \delta E_1 & & \delta E_2 & & \delta E_3 & \\
\text{energy:} & 0 & & \Delta E_1 & & \Delta E_2 & & \Delta E_3
\end{array} \tag{9}$$

In this representation, we associate a change in Coulomb energy δE_i with the ith tunneling event and a net change in Coulomb energy $\Delta E_i=\Sigma_{j=1}^{i}\delta E_j$ with the partially completed process. These Coulomb energies determine the energy barrier for multijunction cotunneling and are the primary factors fixing the associated transition rate. The δE_i can be computed from the electrostatics of the pump's capacitance network, given the initial and final charge states.

Because the order of the single-junction tunneling events $(j_1,\ldots,j_m)$ does not affect the final state, all $m!$ permutations of the set $\{j_1,\ldots,j_m\}$ contribute to the rate of transition from n to n'. In the approximation of Jensen and Martinis,[31] the contribution to the transition rate from this set of mth-order processes is

$$\Gamma^{(m)}_{n'n}=\frac{2\pi}{\hbar}\left(\frac{R_K}{(2\pi)^2R_J}\right)^m S^2F_m(\Delta E_m,T), \tag{10}$$

where

$$S=\sum_{\mathrm{perm}\{j_1,\ldots,j_m\}}\prod_{i=1}^{m-1}\left(\Delta\tilde{E}_i-\frac{i}{m}\Delta E_m\right)^{-1}, \tag{11}$$

$$F_m(\Delta E_m,T)=\frac{-\Delta E_m/(2m-1)!}{1-\exp(\Delta E_m/k_BT)}\times\prod_{i=1}^{m-1}[(2\pi ik_BT)^2+(\Delta E_m)^2], \tag{12}$$

and, following Kautz *et al.*,[6]

$$\Delta\tilde{E}_i=\max(\Delta E_i,k_BT,\Delta E_m+k_BT). \tag{13}$$

Practical implementation of the orthodox theory outlined in Eqs. (7)–(13) requires that consideration be restricted to a finite number of states and cotunneling processes. In the following, the island charges are assumed to be 0 or $\pm e$, so that no more than $3^6=729$ states are considered for a seven-junction pump. Also, following Jensen and Martinis,[31] we omit cotunneling processes of order $m>N$, processes in which tunneling occurs more than once in a given junction, and processes that involve tunneling in both the forward and reverse directions. Under these assumptions, Eqs. (7)–(13) provide a practical method for computing leakage and counting errors in the noise-free pump.

B. Simulations

Extension of the orthodox theory to include noise-induced tunneling is simply a matter of adding the rate given by Eq. (4) to the first-order orthodox rate. Specifically, we assume that

$$\Gamma^{(1)}_{n'n}=\frac{-\Delta E/e^2R_J}{1-\exp(\Delta E/k_BT)}+\frac{\pi\alpha}{2R_J\Delta E}\theta(\Delta E-k_BT), \tag{14}$$

where ΔE is the difference in electrostatic energy between states n' and n and θ denotes the unit step function. This modification adds single-photon, single-junction noise processes but neglects higher-order processes, as appropriate in the limit of weak noise. Equation (14) also neglects correlations between the noise on neighboring junctions, contrary to experimental evidence.[14,15] Nonetheless, Eq. (14) provides a useful first approximation, and we now apply it to estimate the effect of noise on leakage and counting errors in the pump.

The absolute leakage current I_A is experimentally measured for the equilibrium state of a pump with all biases set to zero: $V_E=0$ and $Q_1=Q_2=\cdots=Q_{N-1}=0$. Under these conditions,

$$\frac{dP_n}{dt}=0, \tag{15}$$

and Eq. (7) becomes a set of linear equations that can be solved for the occupation probabilities P_n. However, I_A does not correspond to the current through a junction and cannot be evaluated using Eq. (8). Instead, $I_A=I_++I_-$, where I_+ and I_- are the absolute values of the currents corresponding to processes that transfer a charge through the entire pump in the forward and reverse directions. Evaluation of I_A thus requires enumeration of all possible through processes and calculation of the current associated with each. Suppose that a through transfer consists of K cotunneling processes that take the pump from an initial state n_0 through the successive states $n_1,\ldots,n_K$, where the final state n_K necessarily coincides with the initial state. In this case, the forward and reverse leakage currents can be evaluated as[6]

$$I_\pm=e\sum_{\substack{\text{through}\\ \text{transfers}}} P_{n_0}\Gamma^\pm_{n_1n_0}\prod_{j=2}^{K}\frac{\Gamma^\pm_{n_jn_{j-1}}}{\Gamma_T(n_{j-1})}, \tag{16}$$

where the product is understood to be 1 when $K=1$, Γ^+ and Γ^- are cotunneling rates for the forward and reverse directions, and $\Gamma_T(n)$ is the total rate for exiting state n,

$$\Gamma_T(n)=\sum_{n'\neq n}\Gamma_{n'n}. \tag{17}$$

In Eq. (16), the specified sum over through transfers includes values of K from 1 to N, allowing transfers ranging from a single N-junction cotunneling process to N separate single-junction processes. Also, the sum includes all initial states n_0, but, to avoid double counting, terms are included only if the probabilities of all intermediate states $n_1,\ldots,n_{K-1}$ are less than P_{n0}. This restriction is necessary because the states of a through transfer form a cycle, $n_0\rightarrow n_1\cdots\rightarrow n_{K-1}\rightarrow n_0$, and only one state can be chosen as the initial/final state. Thus, while evaluation of the absolute leakage current is somewhat complicated, the only data required are the steady-state probabilities P_n and the rate matrices $\Gamma^+_{n'n}$ and $\Gamma^-_{n'n}$ for forward and reverse tunneling.

Experimental and theoretical results for the leakage of a well-characterized seven-junction pump are shown in Fig. 4. Because the circuit parameters for this pump were determined from independent measurements, and the electron temperature was measured directly,[3,5] the only adjustable parameter entering the calculation of I_A is the amplitude $\sqrt{\alpha}$ of the $1/f$ noise. In the absence of noise ($\sqrt{\alpha}=0$), the simulation correctly predicts the exponential increase in I_A at temperatures above about 140 mK, but fails to account for the nearly temperature independent leakage observed experimentally at temperatures below about 80 mK. At 35 mK, the discrepancy between the noise-free theory and experiment is almost 19 orders of magnitude. As discussed elsewhere,[6] the $\sqrt{\alpha}=0$ curve is dominated by processes involving N single-junction tunneling events at temperatures above about 60 mK and dominated by processes involving one Nth-order cotunneling event at lower temperatures. When the noise amplitude is suitably adjusted, however, we obtain a rough fit to both the high- and low-temperature portions of the experimental curve. Moreover, the noise amplitude that gives the best fit $\sqrt{\alpha}=200$ nV fits within the range of $1/f$ amplitudes typically observed in SET's, 30–3000 nV. Thus, photon-assisted tunneling driven by $1/f$ noise provides a possible explanation for the experimentally observed leakage below 80 mK. The $\sqrt{\alpha}=50$ nV curve is included in Fig. 4 for comparison because this noise amplitude provides the best explanation for the observed counting errors, as described in the following section.

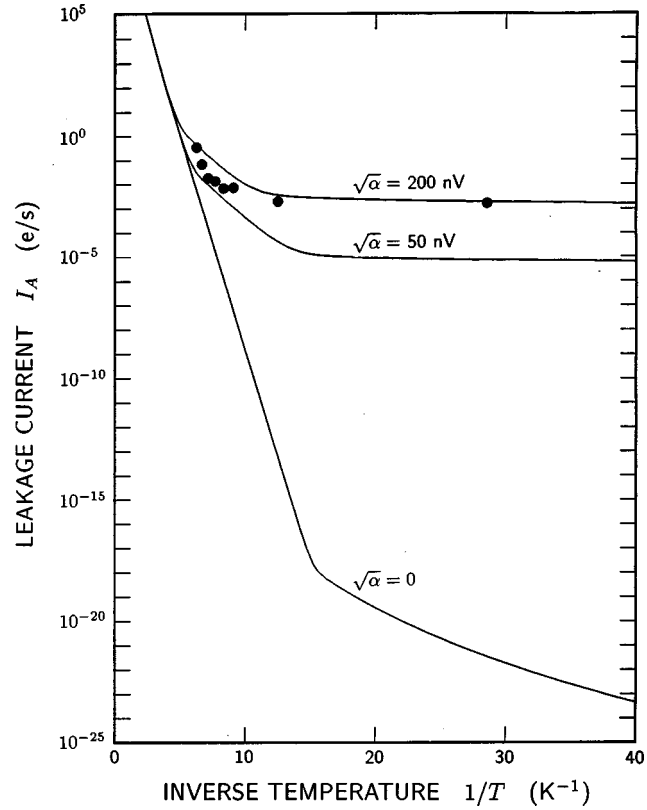

FIG. 4. Absolute leakage current I_A as a function of inverse temperature for a seven-junction pump. Experimental data (circles) are from Ref. 3. Theoretical curves are shown for three noise amplitudes. The pump parameters are $R_J=470\,\mathrm{k\Omega}$, $C_J=0.22$ fF, and $C_g=0.05$ fF.

Experimental data on leakage is also available for pumps with four, five, and six junctions within the temperature regime below about 80 mK, where I_A is nearly constant.[5,22,23] These values are listed in Table I, along with the noise amplitude required to explain the leakage. As might be expected, I_A decreases monotonically with increasing number

TABLE I. Experimental absolute leakage current I_A in the temperature-independent regime below about 80 mK for four electron pumps and the theoretical noise amplitudes $\alpha^{1/2}$ required to account for the leakage. Experimental data are from Refs. 5, 22, and 23.

N	R_J (kΩ)	C_J (fF)	C_g (fF)	T (mK)	I_A (10^{-3} e/s)	$\sqrt{\alpha}$ (nV)
4	460	0.2	0.11	67	480	7.7
5	300	0.2	0.2	40	100	3
6	670	0.2	0.09	67	12	26
7	470	0.22	0.05	33	0.3–2	120–200

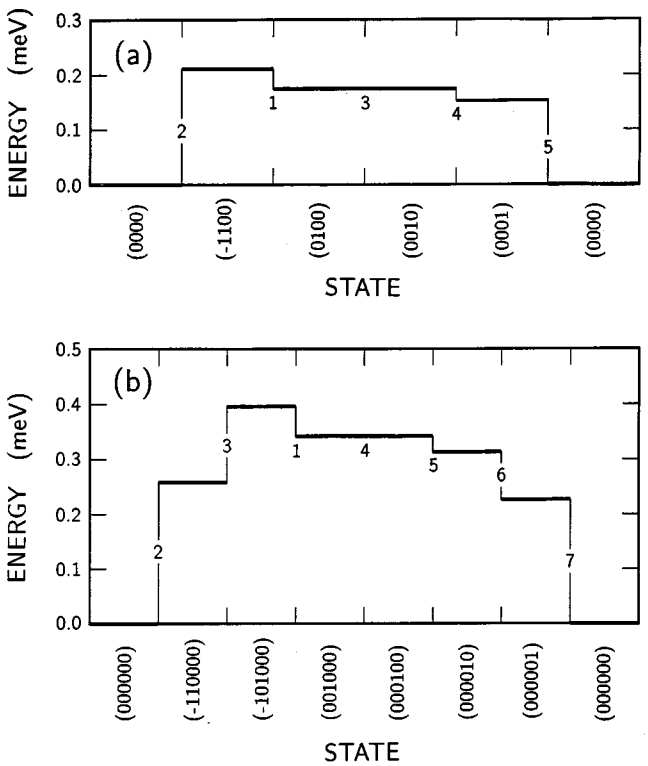

FIG. 5. Electrostatic energy of the intermediate states for typical dominant leakage processes in the (a) five-junction and (b) seven-junction electron pumps. States are labeled by the island charges $(q_1 q_2 \cdots q_{N-1})$ in units of e, and each transition is labeled by the number of the active tunnel junction. Parameters are $C_J = C_g = 0.2$ fF for the five-junction pump and $C_J = 0.22$ fF and $C_g = 0.05$ fF for the seven-junction pump.

of junctions. More important, all of the required noise amplitudes fall close to the range expected from the $1/f$ noise observed in SET's at 10 Hz. Although the noise required to explain leakage in the five-junction pump is an order of magnitude less than that seen in SET's, the deviation is not surprising given that we have extrapolated across 9 orders of magnitude in frequency. Certainly, the similarity of the α values for different pumps supports the proposed explanation of low-temperature leakage in terms of $1/f$ noise.

Insight into the mechanism of noise-induced leakage can be gained by examining the dominant leakage processes in more detail. Analysis of the computation reveals that, in the pumps considered here, all of the dominant processes involve only single-junction tunneling, with negligible contributions from cotunneling. Typical dominant processes for the five- and seven-junction cases are illustrated in Figs. 5(a) and 5(b) in terms of the electrostatic energies of the charge states involved. Each diagram lists the successive states, labeled by the island charges $(q_1 q_2 \cdots q_{N-1})$ in units of e, occupied in the particular leakage process, and plots the corresponding electrostatic energy. Transitions between states are labeled by the number of the active junction. Thus, in Fig. 5(a), the first tunneling occurs in junction 2, takes the pump from charge state (0000) to (-1100), and requires an energy of 0.21 meV. Because this first tunneling requires energy, while the final four do not, we see that leakage in the five-junction pump needs only one photon-assisted tunneling. On the other hand, Fig. 5(b) reveals that leakage in the seven-junction pump requires two photon assists, so it is not surprising that the leakage rate is much lower for seven than for five junctions.

Approximate formulas for the leakage due to the dominant processes can be derived from Eq. (16) using simple limits for the single-junction tunneling rate. In particular, if $|\Delta E| \gg k_B T$ then Eq. (14) can be written as

$$\Gamma^{(1)}_{n'n} = \begin{cases} \dfrac{|\Delta E|}{e^2 R_J} & (\Delta E \ll -k_B T), \\ \dfrac{\pi \alpha}{2 R_J |\Delta E|} & (\Delta E \gg k_B T), \end{cases} \tag{18}$$

so that the tunneling is conventional for ΔE negative and photon assisted for ΔE positive. If the changes in energy for the first two transitions in Fig. 5(a) are taken as ΔE_1 and ΔE_2, then Eq. (16) yields for the five-junction process

$$I_5 \approx \frac{\pi e \alpha}{2 R_J |\Delta E_1|} \left(\frac{|\Delta E_2|}{|\Delta E_1| + |\Delta E_2|} \right), \tag{19}$$

where the first factor is the photon-assisted tunneling current from (0000) to (-1100), the second factor is the probability of tunneling from (-1100) to (0100) rather than back to (0000), and we have assumed that the final tunnelings occur with probability 1. Using Eq. (19) with $\Delta E_1 = 0.211$ meV, $\Delta E_2 = -0.036$ meV, and parameters from Table I, we obtain $I_5 = 0.2\, e/\mathrm{s}$, in rough agreement with the full calculation, which yields $0.023\, e/\mathrm{s}$ for this process. Similarly, for the seven-junction pump, Eq. (16) yields

$$I_7 \approx \frac{\pi e \alpha}{2 R_J |\Delta E_1|} \left(\frac{\pi e^2 \alpha}{2 |\Delta E_1| |\Delta E_2|} \right) \left(\frac{|\Delta E_3|}{|\Delta E_2| + |\Delta E_3|} \right), \tag{20}$$

where the second factor is the probability of photon-assisted tunneling from state (-110000) to (-101000) before the pump can return to state (000000) by conventional tunneling. As expected, the fact that two photons are required leads to a leakage proportional to α^2 and a significantly lower rate than for the five-junction pump. Evaluating Eq. (20) for $\Delta E_1 = 0.259$ meV, $\Delta E_2 = 0.137$ meV, $\Delta E_3 = -0.054$ meV, $\sqrt{\alpha} = 200$ nV, and the tabulated parameters for the seven-junction pump yields $I_7 = 1.6 \times 10^{-3}\, e/\mathrm{s}$, in comparison with $4.6 \times 10^{-5}\, e/\mathrm{s}$ for the full calculation. While Eqs. (19) and (20) are highly approximate (because they overestimate the probability of completing the final tunneling steps), they do include the primary parameter dependencies of the leakage current. In particular, they account for the absence of a temperature dependence and the respective α and α^2 noise dependencies obtained in the full calculation.

IV. COUNTING ERRORS

Two different measures of counting errors have been considered. The simplest is the net charge error $\mathcal{E}_Q = \| Q|/e - 1|$, or the absolute difference between the average charge Q and expected charge e transferred during a pump cycle. $\mathcal{E}_Q$ is a direct measure of the accuracy of an electron pump used as a current standard and has been calculated by several authors for a variety of situations.[31,34–37] However, the most stringent experimental tests of pump accuracy have recorded the infrequent errors, whether positive or negative, occurring

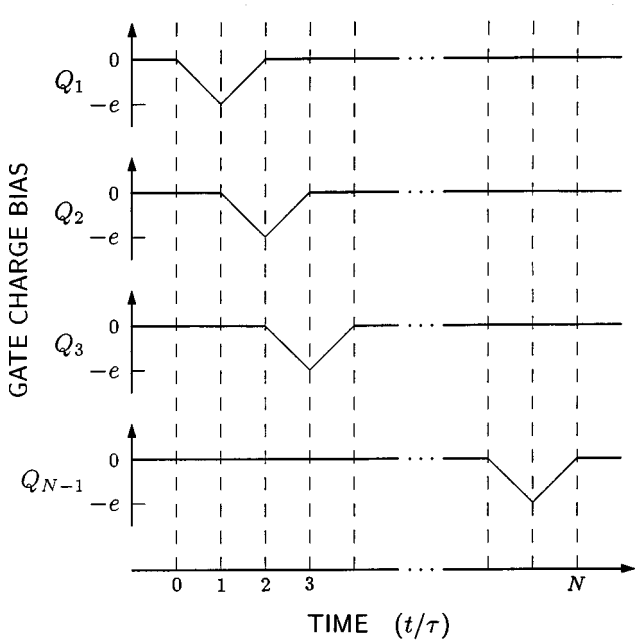

FIG. 6. Charge biases applied to the $N-1$ gates of an N-junction pump to transfer a charge e through the pump.

while the pump is used to shuttle one or two electrons repeatedly back and forth.[3,5,6,23] The shuttle test records an error either if extra charges are transferred or if there is a failure to transfer a charge during a pump cycle. The shuttle error can be expressed as $\mathcal{E}_S=(Q_+ + Q_-)/e$, where $Q_+ \geqslant 0$ is the average extra charge transferred, and $Q_- \geqslant 0$ is the average charge deficit. In these terms, the net charge error is $\mathcal{E}_Q=|Q_+ - Q_-|/e$, so $\mathcal{E}_S$ is an upper bound on $\mathcal{E}_Q$. Indeed, the bias voltage V_E across the pump can be adjusted to produce a cancellation between positive and negative errors that yields $\mathcal{E}_Q=0$, but the shuttle error is never zero. Here we focus on the shuttle error to facilitate comparison with experimental shuttle-error measurements.

Operation of the electron pump requires application of a charge bias to each of the islands in succession. In the experiments considered here, the islands are biased with triangular pulses of duration 2τ, as shown in Fig. 6, and the pumping cycle for the N-junction pump is completed in a time $N\tau$. The succession of pulses causes a single charge to tunnel from island to island until the charge is transferred through the entire pump. This process is illustrated in Fig. 7, which plots the electrostatic energy as a function of the position of a single additional charge at various times during the bias cycle. Initially all the gate biases are zero, and placing an additional charge on any island requires an energy of at least 0.15 meV, so no charge is likely to enter the pump. This situation corresponds to the hold mode in which the Coulomb blockade prevents current flow. However, as a negative bias is applied to the first island, the electrostatic energy associated with an extra charge on the island is reduced, and tunneling from the input electrode to island 1 becomes likely for $t/\tau > 0.5$. However, once a charge tunnels to island 1, entry of a second charge is blocked by the repulsion of the first. In Fig. 7 this blockage is represented by the dashed line, which plots the electrostatic energy of the pump when a second charge is added, assuming that the first charge

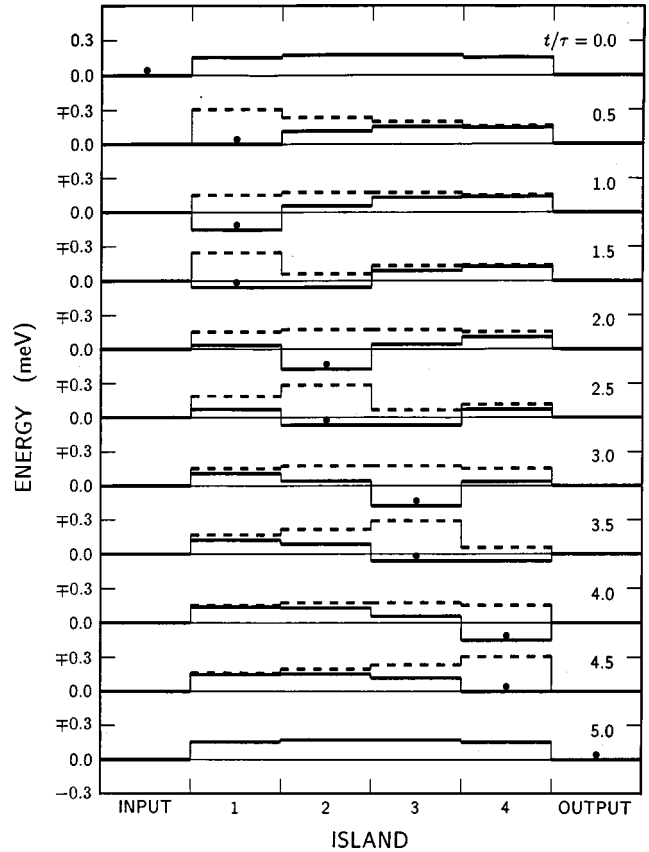

FIG. 7. Electrostatic energy as a function of the location of an extra charge on the four islands of a five-junction pump (solid lines), calculated within the ground-capacitance model for $V_E=0$. Plots are shown at intervals of $\tau/2$ throughout the bias cycle of period 5τ. Dashed lines show the energy when a second extra charge is introduced on successive islands of the pump, with the first extra charge held on the island of minimum energy, as indicated by a filled circle. As the figure illustrates, the pump allows a charge to move from island to island as successive gate charge pulses are applied, but a second charge is prevented from entering the pump by the Coulomb blockade. The pump capacitances are $C_J=C_g=0.2$ fF.

(filled circle) occupies the island of lowest energy. Because energy is required to add a second charge to any of the islands, additional charges are blocked from entering the pump. Pumping action results because a negative charge bias is applied to successive islands, creating an energy well that moves across the pump. The one trapped charge follows the energy minimum, tunneling from island to island, until it is delivered to the output. In effect, the bias schedule creates a moving basket that usually transfers one and only one charge from input to output during each bias cycle.

Although computation of the shuttle error generally requires a separate evaluation of Q_+ and Q_-, in the case of interest here $V_E=0$ and virtually all errors result from the failure of the pump to transfer a charge.[6] Thus, $\mathcal{E}_S \approx 1 - Q/e$ and the shuttle error can be computed by integrating the current through any selected junction during a bias cycle

$$\mathcal{E}_S \approx 1 - \frac{1}{e}\int_0^{N\tau} I_J(t)\,dt. \tag{21}$$

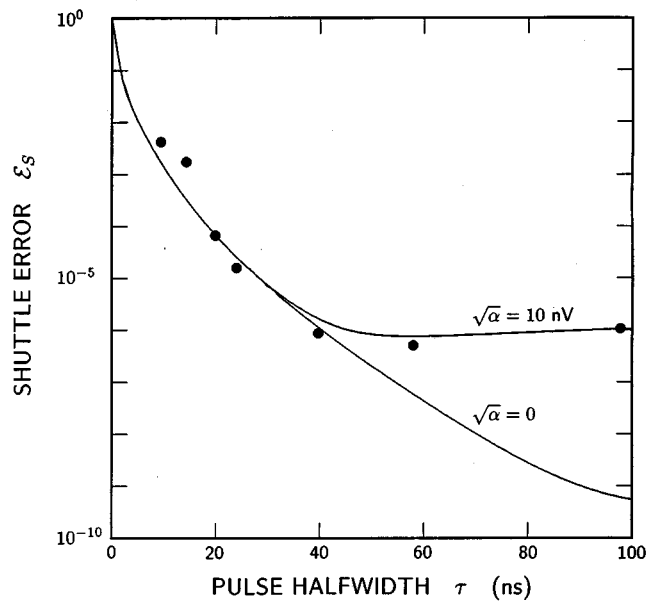

FIG. 8. Shuttle error as a function of pulse halfwidth for a five-junction electron pump. Experimental data (filled circles) are from Ref. 23. Simulations are plotted with and without $1/f$ noise: $\alpha^{1/2} = 10$ nV and 0. Pump parameters are $R_J = 300\,\mathrm{k\Omega}$, $C_J = C_g = 0.2$ fF, and $T = 40$ mK.

To obtain $I_J(t)$, we apply Eq. (8) after integrating Eq. (7) for the bias schedule shown in Fig. 6. In practice, it is important to extend the integration interval somewhat beyond $N\tau$ to eliminate transiently stored charge. Because $\mathcal{E}_S$ is determined by a small difference between two numbers close to 1, we use 33 digit arithmetic to assure accuracy. Convergence was also aided by using a fourth-order semi-implicit Rosenbrock integration method.[38] This method proved essential in some instances due to the stiff nature of the differential equation.

A. Five-junction pump

Experimental and theoretical results for the shuttle error in a five-junction electron pump are shown as a function of pulse halfwidth τ in Fig. 8. The parameters of the five-junction pump were not fully determined, but we know that $R_J = 300\,\mathrm{k\Omega}$ and that C_Σ, the sum of the junction capacitance and its external shunting capacitance, is about 0.4 fF for a typical junction.[23] Thus, the theoretical curves in Fig. 8 were fit to the experiment by adjusting two parameters C_J/C_g and α, with the average C_Σ held fixed. In the absence of noise, $\sqrt{\alpha} = 0$, one can obtain a good fit to the initial slope of the experimental error curve, but it is difficult to account for the flat region observed for $\tau > 40$ ns. However, when noise is included, a good fit is obtained over the entire range of pulse half widths. Moreover, the required noise amplitude of $\sqrt{\alpha} = 10$ nV is comparable to the 3 nV needed to explain leakage in the same device. Thus, introducing $1/f$ noise produces a consistent explanation of both leakage and counting errors in the five-junction pump.

As described previously,[23] counting errors at small τ result because insufficient time is allowed for tunneling and the charge is not transferred through the entire pump. On the other hand, from Fig. 8 we conclude that the error is dominated by noise-induced tunneling for τ greater than about 40 ns. What is the detailed mechanism of the noise-induced errors? Analysis of the computation reveals that two distinct mechanisms contribute equally to errors at large τ. The simpler of the two can be understood from the energy diagram for $t/\tau = 2.5$ in Fig. 7. Just before the charge tunnels from island 2 to 3, a photon assist can provide the energy needed for the charge to tunnel back to island 1, from which the input electrode can be reached without further added energy. Because a second photon assist would be required for the charge to return from the input to island 2, the moving energy well is likely to remain empty for the duration of the bias cycle, and no charge is pumped. Thus, photon-assisted tunneling can cause errors by allowing the charge being pumped to escape back to the input electrode.

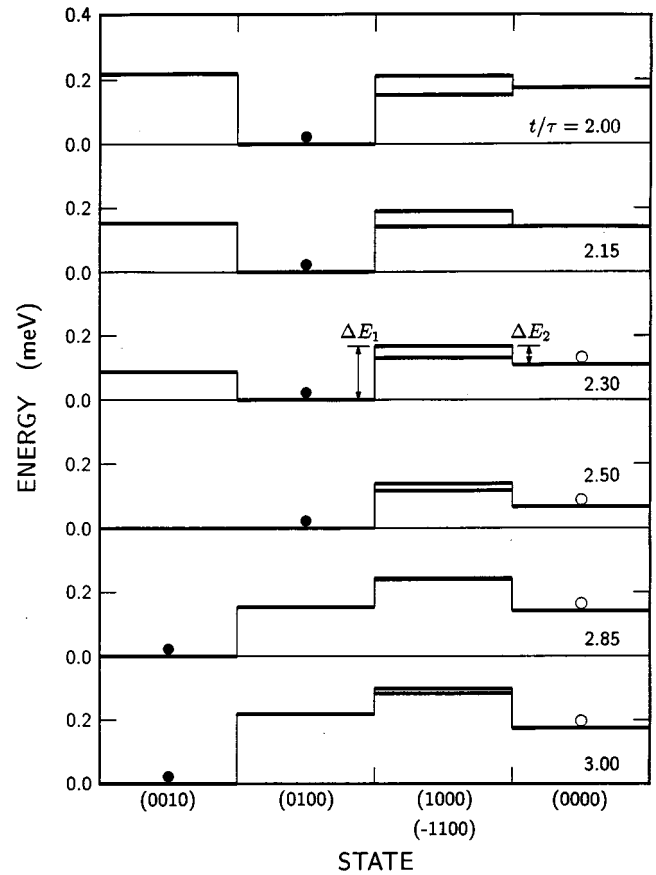

FIG. 9. Electrostatic energy as a function of charge state for selected states of the five-junction pump at various times between $t/\tau = 2$ and 3. The pump can move between adjacent states by tunneling in a single junction. Filled circles identify the state most probably occupied during normal pump operation. Open circles identify the state occupied when errors occur by photon-assisted escape to the input electrode. Pump parameters are $C_J = C_g = 0.2$ fF.

The charge-escape error mechanism can be understood in more detail from the energy diagram shown in Fig. 9. This diagram plots the electrostatic energy of the relevant states, with the states arranged such that transitions between contiguous states require a single tunneling. The filled circle identifies the state most probably occupied during normal pump operation, and the open circle identifies the state occupied in the event of an error. Charge escape occurs when

photon-assisted tunneling moves the pump from the (0100) state to either of the intermediate states (1000) or (-1100), and the intermediate state decays to the (0000) state. At $t/\tau=2$, charge escape is a transient phenomenon since the process (0000)→(-1100)→(0100) does not require energy and quickly restores the charge. For $t/\tau>2.15$, however, this reverse process is blocked by an energy barrier, and charge escape generally leads to an error. But charge escape is possible only for a limited time, since for $t/\tau>2.5$ the charge moves from island 2 to island 3, shifting the state of principal occupation from (0100) to (0010), and escape can no longer occur with a single photon assist.

An approximate formula for the probability P_e of charge escape through the process (0100)→(1000)→(0000) can be written in terms of the energies ΔE_1 and ΔE_2 identified in Fig. 9. Using Eq. (18), we obtain $\pi\alpha/2R_J|\Delta E_1|$ for the rate of photon-assisted tunneling from (0100) to (1000) and $|\Delta E_2|/(|\Delta E_1|+|\Delta E_2|)$ for the probability of a transition (1000) to (0000). Thus, the probability of escape during the interval $2.15<t/\tau<2.5$ is approximately

$$P_e \approx \frac{\pi\alpha}{2R_J}\int_{2.15\tau}^{2.5\tau}\frac{|\Delta E_2|/|\Delta E_1|}{|\Delta E_1|+|\Delta E_2|}dt \qquad (k_BT \ll e^2/C_J, \tau \gg R_JC_J, C_J/C_g=1). \tag{22}$$

An exactly similar formula results for escape by the process (0100)→(-1100)→(0000) with ΔE_1 and ΔE_2 appropriately redefined. Because ΔE_1 and ΔE_2 vary linearly with time over the integration interval, Eq. (22) can be reduced to a closed-form expression for the error probability. Even as written, however, we can conclude from Eq. (22) that the error rate is directly proportional to the noise power α.

The second mechanism for noise-induced errors can also be understood from the energy diagram for $t/\tau=2.5$ in Fig. 7. As the dashed curve in this diagram shows, a single photon assist will allow a second charge to tunnel from the output electrode to island 4 of the pump. Once on island 4, this charge can tunnel without additional energy to island 3, where it becomes trapped, because an additional photon is required to return it to island 4. While the presence of a second charge on island 3 might seem innocuous, it blocks the first charge from tunneling from island 2 to 3, and eventually forces the first charge to return to the input, causing an error.

Details of the charge-blocking error mechanism are shown in Fig. 10. As with charge escape, the key to charge blocking is a photon-assisted step that occurs between $t/\tau=2.15$ and 2.5. In this case, the photon assist takes the pump from the (0100) state to either (011-1) or (0101), after which it can tunnel to the (0110) state without additional energy. In the (0110) state islands 2 and 3 both have an extra charge, and further tunneling is prevented until after $t/\tau=2.85$, when the charge on island 1 returns to the input electrode by the process (0110)→(1010)→(0010). At the end of this charge blocking process, the pump is in the (0010) state, just at it would be during normal pump operation, but the charge on island 3 has come from the output rather than the input.

The key step in the charge-blocking mechanism is the photon-assisted transition from the (0100) state to (0110) via the intermediate state (011-1) or (0101). These processes are

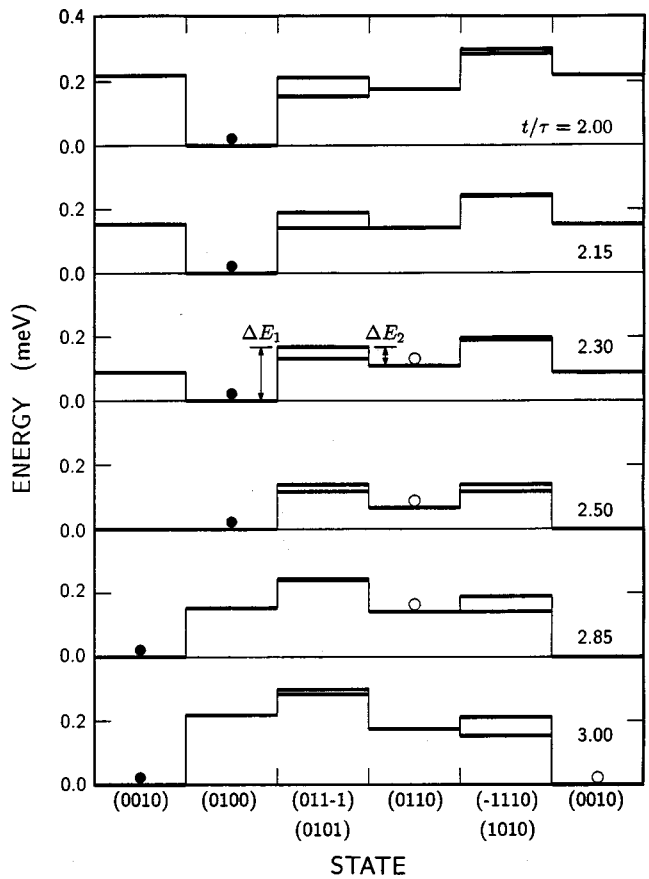

FIG. 10. Electrostatic energy as a function of charge state for selected states of the five-junction pump at various times between $t/\tau=2$ and 3. The pump can move between adjacent states by tunneling in a single junction. Filled circles identify the state most probably occupied during normal pump operation. Open circles identify the states occupied when errors occur by the charge-blocking mechanism. Pump parameters are $C_J=C_g=0.2$ fF.

exactly similar to those that give rise to charge escape and are also governed by Eq. (22) with appropriate energy differences ΔE_1 and ΔE_2. In fact, the energy differences for the charge-blocking process with intermediate state (011-1) are identical to those for the charge-escape process with intermediate state (1000), and the process with intermediate states (0101) and (-1100) are similarly paired. Thus, within the approximation of Eq. (22), the charge-blocking and charge-escape mechanisms contribute equally to the shuttle error. For the particular pump considered here, evaluation of Eq. (22) for all four processes yields

$$\mathcal{E}_S \approx 2.6\frac{\alpha\tau C_J}{e^2R_J} \quad (k_BT \ll e^2/C_J, \tau \gg R_JC_J, C_J/C_g=1). \tag{23}$$

Evaluated for $\tau=100$ ns and the parameters listed in Fig. 8, Eq. (23) gives $\mathcal{E}_S=6.8\times10^{-7}$, in comparison with 1.05×10^{-6} for the full calculation. Thus, Eq. (23) gives a good estimate of the noise-induced errors in the limit of large τ and low T. This formula suggests that errors in the five-junction pump can be reduced by reducing either α or C_J or by increasing R_J, but, because $\mathcal{E}_S$ depends linearly on these

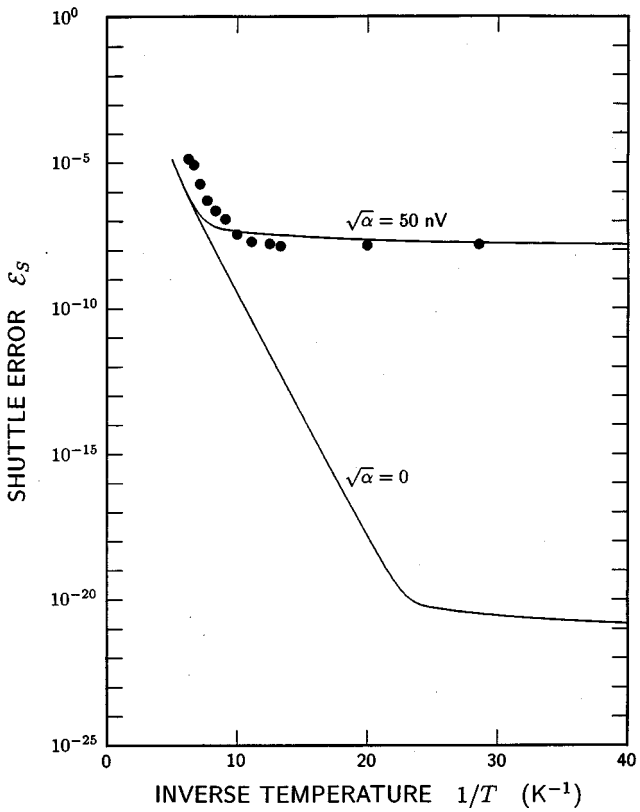

FIG. 11. Shuttle error as a function of inverse temperature for a seven-junction electron pump. Experimental data (filled circles) are from Ref. 3. Simulations are plotted with and without $1/f$ noise: $\alpha^{1/2}=50$ nV and 0. Pump parameters are $R_J=470\,\mathrm{k\Omega}$, $C_J=0.22$ fF, $C_g=0.05$ fF, and $\tau=40$ ns.

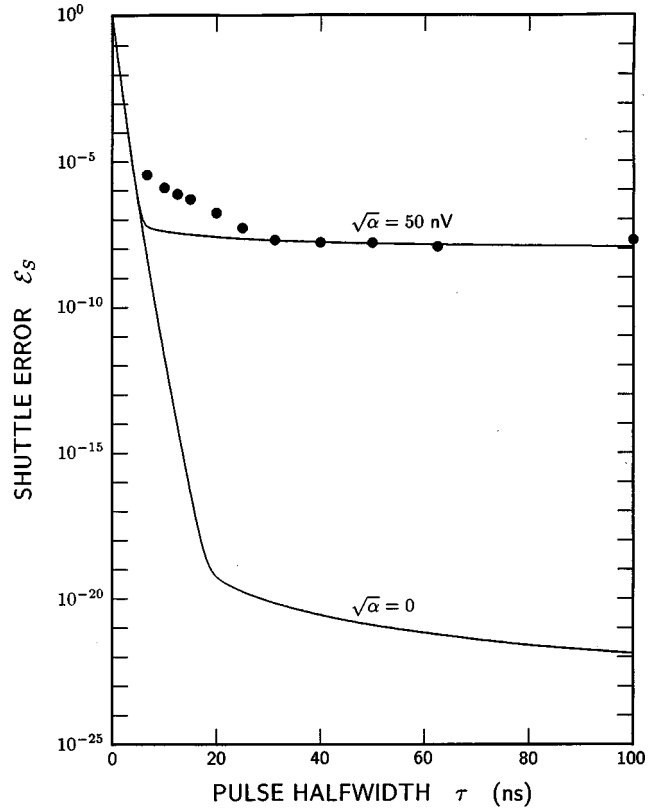

FIG. 12. Shuttle error as a function of pulse halfwidth for a seven-junction electron pump. Experimental data (filled circles) are from Ref. 3. Simulations are plotted with and without $1/f$ noise: $\alpha^{1/2}=50$ nV and 0. Pump parameters are $R_J=470\,\mathrm{k\Omega}$, $C_J=0.22$ fF, $C_g=0.05$ fF, and $T=33$ mK.

quantities, significant reductions in $\mathcal{E}_S$ may be difficult to achieve. A more promising approach is to increase the number of junctions.

B. Seven-junction pump

The particular seven-junction pump considered here has been the subject of extensive experiments, and all pump parameters were directly measured.[3,5,6] As a result, the only parameter adjusted to fit theoretical curves to the experimental shuttle error is the noise amplitude $\sqrt{\alpha}$. As can be seen from Fig. 11, which plots $\mathcal{E}_S$ as a function of inverse temperature for $\tau=40$ ns, a noise amplitude of 50 nV yields a good fit to the experimental data for the seven-junction pump. As in the five-junction case, this amplitude is comparable to the value of 200 nV required to explain leakage in the same device. More important, by introducing a modest level of noise, we are able explain the discrepancy of more than 12 orders of magnitude between the experimental shuttle error at 33 mK and the noise-free theory. Indeed, including noise provides a good fit to $\mathcal{E}_S$ over the entire range of experimental temperatures.

As noted previously,[6,31] the extremely low error rates predicted by the noise-free theory for $\tau>20$ ns are due to cotunneling of order $N-1$. When noise is included, however, the errors contributed by such high-order effects are entirely insignificant, and cotunneling can be omitted from the calculation. With this understanding, future analyses of leakage and counting errors in the pump can be significantly simplified.

Figure 12 compares the experimental and theoretical shuttle error as a function of pulse half width at 33 mK. In this case, including noise yields good agreement with experiment for $\tau>30$ ns, where $\mathcal{E}_S$ is nearly independent of τ, but the theory fails to reproduce the exponential dependence of $\mathcal{E}_S$ observed experimentally for $\tau<30$ ns. To its credit, noise-induced tunneling does explain the 14-orders-of-magnitude discrepancy between the experimental error at $\tau=100$ ns and the noise-free prediction. The remaining discrepancy for $\tau<30$ ns suggests than errors at small pulse halfwidths are due to an unknown mechanism.

Disregarding the problem of small τ for the moment, we first consider the physical origin of noise-induced errors in the limit of large τ and low T. As noted previously,[6] the exponential dependence of $\mathcal{E}_S$ on $1/T$ observed for $T>100$ mK is due to a thermally activated escape mechanism analogous to the photon-assisted escape described for the five-junction pump in the previous section. Thus, noise-induced errors are important only in the limit of large τ and low T, but this is the parameter region of greatest interest because it yields the lowest error.

Insight into the mechanism of noise-induced errors is provided by Fig. 13, which plots the electrostatic energy at various times near the middle of the bias cycle. A possible mechanism is suggested by the plot for $t/\tau=3.5$, which

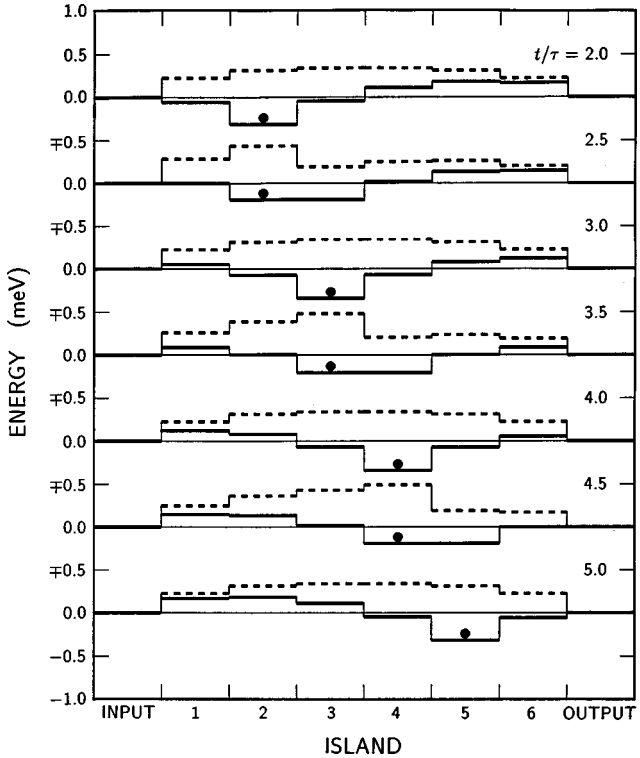

FIG. 13. Electrostatic energy as a function of the location of an extra charge on the six islands of a seven-junction pump (solid lines), calculated within the ground-capacitance model for $V_E=0$. Plots are shown at intervals of $\pi/2$ for the middle portion of the bias cycle. Dashed lines show the energy when a second extra charge is introduced on successive islands of the pump, with the first extra charge held on the island of minimum energy, as indicated by a filled circle. The pump capacitances are $C_J=0.22$ fF and $C_g=0.05$ fF.

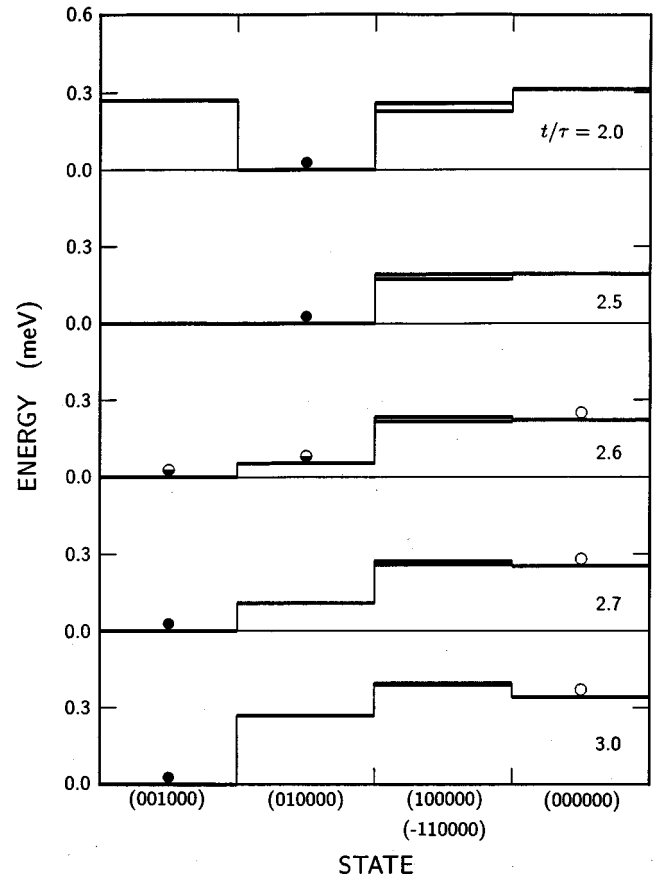

FIG. 14. Electrostatic energy as a function of charge state for selected states of the seven-junction pump at various times between $t/\tau=2$ and 3. The pump can move between adjacent states by tunneling in a single junction. Filled circles identify the state most probably occupied during normal pump operation, while partially filled circles show an incomplete transition between normally occupied states. Open circles identify the state occupied when errors occur by photon-assisted escape to the input electrode. Pump parameters are $C_J=0.22$ fF and $C_g=0.05$ fF.

shows that both charge escape and charge blocking are possible if photon-assisted tunneling is used to surmount two energy barriers. If this were the dominant error process, and the energy barriers are taken as ΔE_1 and ΔE_2, then the error rate for the seven-junction pump would be less than for five junctions by a factor of roughly $p=\pi e^2\alpha/(2|\Delta E_1||\Delta E_2|)$, which is the probability of surmounting the second barrier once the first barrier is surmounted [see Eqs. (19) and (20)]. Evaluating this factor for $\sqrt{\alpha}=50$ nV and the barriers at $t/\tau=3.5$, we obtain $p=2\times10^{-7}$, indicating that the error rate for 7 junctions should be dramatically less than for five junctions if two photons are required to create an error.

Unfortunately, errors in the seven-junction pump are actually dominated by processes that require just one photon. In particular, the charge being pumped can escape from the energy well during a brief period after $t/\tau=2.5$ using only one photon. Details of this process are shown in Fig. 14, which plots the energy levels for the relevant states. At $t/\tau=2.5$, the energy of the (001000) state equals that of the (010000) state, and the charge on island 2 can begin tunneling to island 3. Also at $t/\tau=2.5$, the energy of the (100000) state is by coincidence nearly equal to that of the (000000) state, and afterwards the charge being pumped can escape to the input by photon-assisted tunneling to (100000) followed by ordinary tunneling to (000000). Thus, escape is possible using a single photon during the brief interval while charge remains on island 2. Although the escaped charge can initially leak back to island 2 via the (−110000) state, the small energy difference between the (000000) and (−110000) states makes this process slow, and it is virtually eliminated after $t/\tau=2.65$ when the energy difference is reversed.

How long does the charge stay on island 2 after $t/\tau=2.5$, remaining susceptible to photon-assisted escape? Considering only tunneling from island 2 to island 3 through junction 3, we have, using Eq. (18) in the limit of low temperature,

$$\frac{dP_2}{dt}=-\frac{|\Delta E|}{e^2R_J}P_2, \tag{24}$$

where P_2 is the probability of finding the charge on island 2 and ΔE is the energy difference for the tunneling process. Since $|\Delta E|$ increases linearly from 0 to $e^2/2C_{\Sigma 3}$ during the interval from $t/\tau=2.5$ to 3, we have $|\Delta E|=e^2t'/\tau C_{\Sigma 3}$, where $t'=t-2.5\tau$ and $C_{\Sigma 3}$ is the total capacitance across junction 3. Integration of Eq. (24) thus yields

$$P_2(t')=\exp(-t'^2/2\tau R_J C_{\Sigma 3}). \tag{25}$$

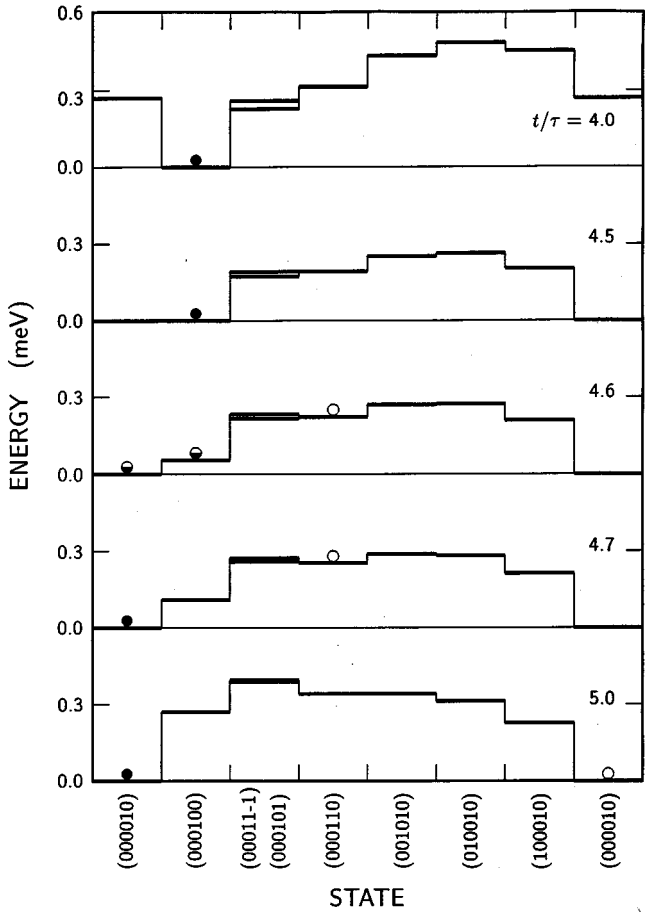

FIG. 15. Electrostatic energy as a function of charge state for selected states of the seven-junction pump at various times between $t/\tau=4$ and 5. The pump can move between adjacent states by tunneling in a single junction. Filled circles identify the state most probably occupied during normal pump operation, while partially filled circles show an incomplete transition between normally occupied states. Open circles identify the state occupied when errors occur by the charge-blocking mechanism. Pump parameters are $C_J=0.22$ fF and $C_g=0.05$ fF.

We conclude from Eq. (25) that escape to the input electrode using a single photon is possible in the seven-junction pump for a time of order $t_7=\sqrt{\tau R_J C_{\Sigma 3}}$. By comparison, in the case of five junctions escape is possible for a time of order τ. Thus, if all else is equal, we can expect errors in the seven-junction pump to be reduced from five junctions by a factor of roughly $t_7/\tau=\sqrt{R_J C_{\Sigma 3}/\tau}$. For the seven-junction parameters, we find $C_{\Sigma 3}=0.30$ fF and $t_7/\tau=0.04$ at $\tau=100$ ns, predicting a modest improvement in error rate between the five- and seven-junction pumps comparable to that obtained experimentally.

When Eq. (25) is combined with approximate transition rates to estimate the error due to charge escape, we find that it accounts for roughly half the errors obtained in the full calculation. The remaining errors are due to a charge-blocking mechanism that contributes equally. For completeness, the energy diagrams for charge blocking, which occurs just after $t/\tau=4.5$, are shown in Fig. 15. In this process, a second charge enters the pump from the output electrode and blocks the charge being pumped from reaching the fifth island. Later, after $t/\tau=5$, the first charge returns to the input, and no charge is pumped.

Can counting errors be reduced below the level of 1.5×10^{-8} obtained with the seven-junction pump? The brief interval over which charge escape or blocking is possible with a single photon suggests that some modification of the bias schedule or parameters of the seven-junction pump might significantly reduce or eliminate errors due to these mechanisms. A limited investigation of this possibility indicates, however, that the single-photon processes are robust and cannot be eliminated from the seven-junction pump with a simple trick. If confirmed by further study, this conclusion implies that a dramatic reduction in errors would require a pump with eight or more junctions. If errors due to single-photon processes could be eliminated, however, the added complexity might be justified since higher-order processes are likely to be several orders of magnitude less frequent, as noted above.

V. SELF-HEATING

In the absence of biases the pump is in thermal equilibrium with its surroundings, and experiments confirm that the electron temperature matches that of the cold stage.[5] Thus, leakage is completely unaffected by self-heating. In the pumping mode, however, energy is dissipated in the islands of the pump whenever tunneling occurs at a voltage beyond threshold. While estimates indicate that the temperature rise due to self-heating is modest,[31,34,39] typically a few tens of millikelvins, we speculate that it might explain the exponential rise in errors observed in the seven-junction pump for pulse half widths less than 30 ns. Self-heating is more important for small τ because tunneling is more likely to occur far from threshold when the pump is operated rapidly [see Eq. (25)]. Thus, self-heating is a good candidate for explaining this otherwise unexplained error regime.

Following earlier work,[31,34,39] we assume that the electron temperature T_i of island i is related to the power $\mathcal{P}_i$ dissipated in the island by

$$T_i^5=T^5+\mathcal{P}_i/\Sigma\Omega, \tag{26}$$

where T is the substrate temperature, Σ is a material constant, and Ω is the volume of the island. Equation (26) applies at low temperatures where the weak coupling between electrons and phonons limits the rate at which energy can be transferred to the substrate. Various values of the parameter Σ have been measured for aluminum,[13,40–42] the island material used here, and we assume a rough average $\Sigma=0.3\,\mathrm{nW/K^5/\mu m^3}$. In adopting Eq. (26), we assume that the electron population of an island always assumes a thermal distribution and can be characterized by a temperature T_i.

In the presence of self-heating, the electrodes of a tunnel junction generally differ in temperature, and Eq. (14) for the tunneling rate must be replaced by a more general formula. In particular, the rate of tunneling from island i to i' is[40]

$$\Gamma_{i'i}=\frac{1}{e^2R_J}\int_{-\infty}^{\infty}f_i(E)[1-f_{i'}(E-\Delta E)]dE + \frac{\pi\alpha}{2R_J\Delta E}\theta(\Delta E-k_BT), \tag{27}$$

where ΔE is the change in electrostatic energy and f_i is the Fermi factor for charges on island i,

$$f_i(E)=\frac{1}{\exp(E/k_BT_i)+1}. \tag{28}$$

While noise-induced tunneling is included in Eq. (27) in a low-temperature limit, this approximation is valid for the cases considered because the relevant energy barriers ΔE are much greater than k_BT even in the presence of self-heating. Furthermore, because noise is included in all self-heating calculations, cotunneling can be neglected, and Eq. (27) defines all transition rates.

In order to evaluate $\mathcal{P}_i$, we compute the average power dissipated in all tunnelings involving island i over one bias cycle. Suppose that in tunneling from island i to i' in Eq. (27) the charge state of the pump changes from n to n'. If the system occupies state n at a given time, then the instantaneous powers dissipated in islands i and i' due to the process $n\rightarrow n'$ are[40]

$$\rho_{n'n}(i)=\frac{1}{e^2R_J}\int_{-\infty}^{\infty}(-E)f_i(E)[1-f_{i'}(E-\Delta E)]dE, \tag{29}$$

$$\rho_{n'n}(i')=\frac{1}{e^2R_J}\int_{-\infty}^{\infty}(E-\Delta E)f_i(E)[1-f_{i'}(E-\Delta E)]dE, \tag{30}$$

and the power dissipated in island i due to all tunnelings averaged over the bias cycle is

$$\mathcal{P}_i=\frac{1}{N\tau}\sum_{n,n'}\int_0^{N\tau}\rho_{n'n}(i)P_ndt, \tag{31}$$

where the sum is understood to include all transitions $n\rightarrow n'$ in which a charge either enters or leaves island i.

Combining Eqs. (7), (26), (27), and (31) with the bias schedule shown in Fig. 6, we can calculate a self-consistent electron temperature T_i for each of the islands along with the shuttle error $\mathcal{E}_s$ in the presence of self heating. Initially we assume that the input and output electrodes and all of the islands are at the substrate temperature T. Integrating over one bias cycle then provides an estimate of the average power $\mathcal{P}_i$ dissipated in each island, and from Eq. (26) we obtain improved estimates for the island temperatures. Because the volumes of the input and output electrodes are large, they are assumed to remain at the substrate temperature. Iterating this procedure for a few bias cycles yields a self-consistent set of T_i and the desired $\mathcal{E}_s$.

The effect of self heating on the five-junction pump is shown in Fig. 16. For this pump the volume of each aluminum island is $\Omega=0.028\,\mu\text{m}^3$, yielding $\Sigma\Omega=8.4\times10^{-12}\,\text{W/K}^5$. Fully self-consistent calculations of the average island temperature and shuttle error are plotted as a function of the pulse half width in Fig. 16 for the original parameter set ($C_J=C_g=0.2\,\text{fF}$), with solid and dashed lines indicating results with and without self-heating. As expected, with self-heating the temperature of the island electrons increases with decreasing pulse width, reaching about 110 mK at $\tau=10\,\text{ns}$. The variation in temperature between islands is slight, with no island differing from the average by more than 3%. As shown in Fig. 16(b), the effect of self-heating on the shuttle error can be significant, increasing the error by about an order of magnitude at $\tau=40\,\text{ns}$. While this increase creates a significant discrepancy between theory and experiment, the fit can be restored by readjusting the junction and gate capacitances. For $C_J=0.23\,\text{fF}$ and $C_g=0.17\,\text{fF}$, we obtain about the same fit with self-heating as previously obtained without. Thus, although self-heating is significant in the five-junction pump, it does not appreciably alter our understanding of the shuttle error.

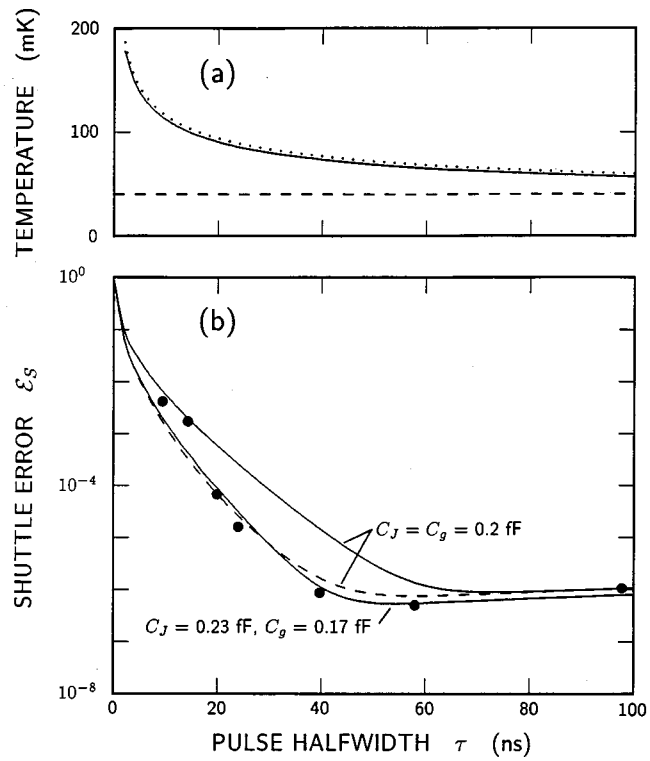

FIG. 16. Average electron temperature (a) and shuttle error (b) as a function of pulse half width for a five-junction electron pump. Solid and dashed lines show results with and without self-heating. The dotted temperature curve corresponds to Eqs. (26) and (33) averaged over islands, while the solid temperature curve is for a self-consistent calculation. Circles show experimental data. Pump parameters are $R_J=300\,\text{k}\Omega$, $\alpha^{1/2}=10\,\text{nV}$, $T=40\,\text{mK}$, $\Sigma\Omega=8.4\times10^{-12}\,\text{W/K}^5$, and the indicated capacitances.

The dotted curve in Fig. 16(a) plots an analytic approximation for the island temperature based on arguments similar to those given previously.[34,39] The approximation is valid in the limit of low temperature, where Eqs. (29) and (30) reduce to $\rho_{n'n}(i)=\rho_{n'n}(i')=(\Delta E^2/2e^2R_J)\theta(-\Delta E)$. An additional simplification results when we recognize that significant energy is dissipated in a given island only twice during a bias cycle: when the charge being pumped tunnels onto the island and when it tunnels off again. But for these processes we can apply the arguments given earlier in regard to Eq. (25) to note that $|\Delta E|=e^2t'/\tau C_\Sigma$, and the probability of remaining in the initial state is $P=\exp(-t'/2\tau R_JC_\Sigma)$, where t' measures time from the tunneling threshold and C_Σ is for the relevant junction. Combining these results with Eq. (31) yields for the average power $\mathcal{P}_i^+$ dissipated when a charge tunnels onto island i,

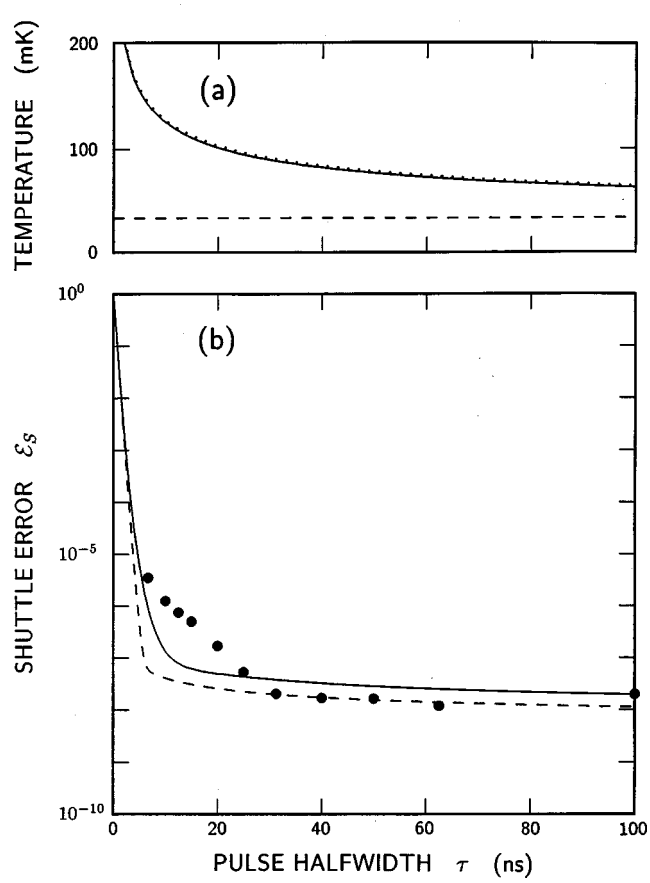

FIG. 17. Average electron temperature (a) and shuttle error (b) as a function of pulse half width for a seven-junction electron pump. Solid and dashed lines show results with and without self-heating. The dotted temperature curve corresponds to Eqs. (26) and (33) averaged over islands, while the solid temperature curve is for a self-consistent calculation. Circles show experimental data. Pump parameters are $R_J = 470\,\mathrm{k\Omega}$, $C_J = 0.22\,\mathrm{fF}$, $C_g = 0.05\,\mathrm{fF}$, $\alpha^{1/2} = 50\,\mathrm{nV}$, $T = 33\,\mathrm{mK}$, and $\Sigma\Omega = 5.4\times 10^{-12}\,\mathrm{W/K^5}$.

$$\mathcal{P}_i^+ = \frac{1}{N\tau}\int_0^{\tau/2} \frac{(e^2 t'/\tau C_{\Sigma+})^2}{2e^2 R_J} \exp(-t'/2\tau R_J C_{\Sigma+})\,dt'$$
$$= \frac{e^2}{2N\tau C_{\Sigma+}}\left(\frac{\pi R_J C_{\Sigma+}}{2\tau}\right)^{1/2}, \tag{32}$$

where the integration interval has been extended to ∞, assuming that $R_J C_{\Sigma+} \ll \tau$. Since the dissipation for a charge leaving island i is exactly similar, the total power, $\mathcal{P}_i = \mathcal{P}_i^+ + \mathcal{P}_i^-$, is

$$\mathcal{P}_i = \sqrt{\frac{\pi}{8}}\left(\frac{e^2 R_J^{1/2}}{N\tau^{3/2}}\right)\left(\frac{1}{C_{\Sigma+}^{1/2}} + \frac{1}{C_{\Sigma-}^{1/2}}\right), \tag{33}$$

where $C_{\Sigma+}$ and $C_{\Sigma-}$ are the total capacitances of the junctions through which the charge enters and leaves the island. Equation (33) extends previous formulas to include the effect of ground capacitance, and, as Fig. 16(a) shows, yields a remarkably accurate prediction of the island temperature compared to the full calculation.

The effect of self-heating on the seven-junction pump is shown in Fig. 17, which plots temperature and shuttle error as a function of pulse half width. For this pump the island volume is $\Omega = 0.018\,\mu\mathrm{m}^3$, yielding a heating coefficient of $\Sigma\Omega = 5.4\times 10^{-12}\,\mathrm{W/K^5}$. As for five junctions, self-heating tends to raise the shuttle error, but in the 7-junction case the increase is nearly constant for $\tau > 15\,\mathrm{ns}$. Although a curve is not shown, the fit to experiment can be restored for $\tau > 40\,\mathrm{ns}$ by reducing the noise amplitude $\sqrt{\alpha}$ from 50 to 40 nV. This adjustment leaves a net increase in the computed $\mathcal{E}_S$ for $\tau < 15\,\mathrm{ns}$, but self-heating clearly does not explain the exponential variation of $\mathcal{E}_S$ with τ observed experimentally for pulse half widths less than 30 ns. Indeed, self-heating does not change any qualitative conclusion of the present study.

VI. CONCLUSION

The leakage and counting errors observed experimentally in the seven-junction pump at low temperatures and low counting rates are many orders of magnitude higher than can be explained by the dynamics of the noise-free system. By including photon-assisted tunneling driven by $1/f$ noise at microwave frequencies, we obtain good agreement between theory and experiment. The required level of noise is consistent with that observed at audio frequencies in SET's. We speculate that the noise responsible for the errors derives from the slow relaxation of charges trapped in metastable states in the dielectric when the device was cooled from room temperature.

In the scenario explored here, the dominant leakage and error processes involve only single-junction tunneling, either conventional or photon assisted, and cotunneling plays no significant role. At low temperatures, leakage in the five-junction pump is dominated by processes that require a single photon-assisted tunneling step, while in the seven-junction pump two photon assists are needed. Counting errors in the limit of low temperatures and low counting rates derive from two types of process: one in which the charge being pumped uses a photon assist to escape back to the input electrode and one in which the charge is blocked by a second charge entering from the output electrode, also with a photon assist. In the five-junction pump these error processes occur over a fixed fraction of the bias-pulse half width, while in the seven-junction pump they occur over a shorter time, related to the RC time of the tunnel junctions. Self-heating during pump operation can raise the temperature of island electrons by several tens of millikelvins, but it generally has a small effect on the rate of noise-induced counting errors.

Two issues related to counting errors remain unresolved. First, the theory presented here does not explain a regime in which errors increase exponentially with counting rate in the seven-junction pump. Understanding this regime is important if the pump is to be operated at high speeds. Second, it is not known whether a pump can be designed, perhaps with more than seven junctions, in which counting errors require two or more photon-assisted tunneling steps. If two photons were needed, a much lower error rate would be expected. Whatever the resolution of these issues, however, the present study demonstrates that noise-induced tunneling is the probable cause of the lowest experimentally observed error rates.

[1] H. Pothier, P. Lafarge, P. F. Orfila, C. Urbina, D. Esteve, and M. H. Devoret, Physica B **169**, 573 (1991); C. Urbina, H. Pothier, P. F. Lafarge, P. F. Orfila, D. Esteve, and M. Devoret, IEEE Trans. Magn. **27**, 2578 (1991); H. Pothier, P. Lafarge, C. Urbina, D. Esteve, and M. H. Devoret, Europhys. Lett. **17**, 249 (1992).
[2] E. R. Williams, R. N. Ghosh, and J. M. Martinis, J. Res. Natl. Inst. Stand. Technol. **97**, 299 (1992).
[3] M. W. Keller, J. M. Martinis, N. M. Zimmerman, and A. H. Steinbach, Appl. Phys. Lett. **69**, 1804 (1996); M. W. Keller, J. M. Martinis, A. H. Steinbach, and N. M. Zimmerman, IEEE Trans. Instrum. Meas. **46**, 307 (1997).
[4] M. W. Keller, A. L. Eichenberger, J. M. Martinis, and N. M. Zimmerman, Science **285**, 1706 (1999).
[5] M. W. Keller, J. M. Martinis, and R. L. Kautz, Phys. Rev. Lett. **80**, 4530 (1998).
[6] R. L. Kautz, M. W. Keller, and J. M. Martinis, Phys. Rev. B **60**, 8199 (1999).
[7] J. M. Martinis and M. Nahum, Phys. Rev. B **48**, 18 316 (1993).
[8] J. D. White and M. Wagner, Phys. Rev. B **48**, 2799 (1993).
[9] G. Zimmerli, T. M. Eiles, R. L. Kautz, and J. M. Martinis, Appl. Phys. Lett. **61**, 237 (1992).
[10] J. M. Hergenrother, M. T. Tuominen, T. S. Tighe, and M. Tinkham, IEEE Trans. Appl. Supercond. **3**, 1980 (1993).
[11] E. H. Visscher, S. M. Verbrugh, J. Lindeman, P. Hadley, and J. E. Mooij, Appl. Phys. Lett. **66**, 305 (1995).
[12] D. Song, A. Amar, C. J. Lobb, and F. C. Wellstood, IEEE Trans. Appl. Supercond. **5**, 3085 (1995).
[13] S. M. Verbrugh, M. L. Benhamadi, E. H. Visscher, and J. E. Mooij, J. Appl. Phys. **78**, 2830 (1995).
[14] A. B. Zorin, F.-J. Ahlers, J. Niemeyer, T. Weimann, H. Wolf, V. A. Krupenin, and S. V. Lotkhov, Phys. Rev. B **53**, 13 682 (1996).
[15] H. Wolf, F. J. Ahlers, J. Niemeyer, H. Scherer, T. Weimann, A. B. Zorin, V. A. Krupenin, S. V. Lotkhov, and D. E. Presnov, IEEE Trans. Instrum. Meas. **46**, 303 (1997).
[16] N. M. Zimmerman, J. L. Cobb, and A. F. Clark, Phys. Rev. B **56**, 7675 (1997).
[17] A. N. Tavhelidze and J. Mygind, J. Appl. Phys. **83**, 310 (1998).
[18] V. A. Krupenin, D. E. Presnov, M. N. Savvateev, H. Scherer, A. B. Zorin, and J. Niemeyer, J. Appl. Phys. **84**, 3212 (1998).
[19] T. Henning, B. Starmark, T. Claeson, and P. Delsing, Eur. Phys. J. B **8**, 627 (1999).
[20] B. Starmark, T. Henning, T. Claeson, P. Delsing, and A. N. Korotkov, J. Appl. Phys. **86**, 2132 (1999).
[21] P. J. Hakonen, J. M. Ikonen, Ü. Parts, J. S. Penttilä, L. R. Roschier, and M. A. Paalanen, J. Appl. Phys. **86**, 2684 (1999).
[22] M. Covington, M. W. Keller, R. L. Kautz, and J. M. Martinis, Phys. Rev. Lett. **84**, 5192 (2000).
[23] J. M. Martinis, N. Nahum, and H. D. Jensen, Phys. Rev. Lett. **72**, 904 (1994); Physica B **194–196**, 1045 (1994).
[24] P. Dutta and P. M. Horn, Rev. Mod. Phys. **53**, 497 (1981).
[25] M. Kenyon, J. L. Cobb, A. Amar, D. Song, N. M. Zimmerman, C. J. Lobb, and F. C. Wellstood, IEEE Trans. Appl. Supercond. **9**, 4261 (1999).
[26] N. M. Zimmerman and W. H. Huber, in *2000 Conference on Precision Electromagnetic Measurements Digest*, edited by J. Hunter and L. Johnson (IEEE, New York, 2000), p. 14.
[27] M. B. Weissman, Rev. Mod. Phys. **60**, 537 (1988).
[28] P. Bak, C. Tang, and K. Wiesenfeld, Phys. Rev. Lett. **59**, 381 (1987); Phys. Rev. A **38**, 364 (1988).
[29] D. V. Averin and K. K. Likharev, in *Mesoscopic Phenomena in Solids*, edited by B. L. Altschuler, P. A. Lee, and R. A. Webb (Elsevier, Amsterdam, 1991), p. 173.
[30] D. V. Averin and A. A. Odintsov, Phys. Lett. A **140**, 251 (1989); Zh. Eksp. Teor. Fiz. **96**, 1349 (1989) [Sov. Phys. JETP **69**, 766 (1989)].
[31] H. D. Jensen and J. M. Martinis, Phys. Rev. B **46**, 13 407 (1992).
[32] L. R. C. Fonseca, A. N. Korotkov, K. K. Likharev, and A. A. Odintsov, J. Appl. Phys. **78**, 3238 (1995).
[33] M. B. A. Jalil, M. Wagner, and H. Ahmed, J. Appl. Phys. **85**, 1203 (1999).
[34] H. Pothier, Ph.D. thesis, University of Paris 6, 1991.
[35] D. V. Averin, A. A. Odintsov, and S. V. Vyshenskii, J. Appl. Phys. **73**, 1297 (1993).
[36] R. W. Rendell, Phys. Rev. B **52**, 4684 (1995).
[37] L. R. C. Fonseca, A. N. Korotkov, and K. K. Likharev, J. Appl. Phys. **79**, 9155 (1996); Appl. Phys. Lett. **69**, 1858 (1996).
[38] W. H. Press, S. A. Teukolsky, W. T. Vettering, and B. P. Flannery, *Numerical Recipes in Fortran*, 2nd ed. (Cambridge, New York, 1992), p. 731.
[39] Q. Niu, C. Liu, H. L. Edwards, A. L. de Lozanne, and W. P. Kirk, IEEE Trans. Instrum. Meas. **44**, 564 (1995); C. Liu and Q. Niu, Phys. Rep. **286**, 349 (1997).
[40] R. L. Kautz, G. Zimmerli, and J. M. Martinis, J. Appl. Phys. **73**, 2386 (1993).
[41] J. P. Kauppinen and J. P. Pekola, Phys. Rev. B **54**, R8353 (1996).
[42] V. A. Krupenin, S. V. Lothkov, H. Scherer, T. Weimann, A. B. Zorin, F.-J. Ahlers, J. Niemeyer, and H. Wolf, Phys. Rev. B **59**, 10 778 (1999).